

# Mixed-Valence Ammonium Trivanadate with a Tunnel Structure Prepared by Pyrolysis of Polyoxovanadate

Haruo Naruke and Toshihiro Yamase\*

Research Laboratory of Resources Utilization, Tokyo Institute of Technology,  
4259 Nagatsuta, Midori-ku, Yokohama 226-8503

(Received June 24, 1999)

The pyrolysis of a polyoxovanadate solid,  $(\text{NH}_4)_{12}[\text{V}_{18}\text{O}_{42}(\text{H}_2\text{O})] \cdot n\text{H}_2\text{O}$  ( $n \approx 11$ ), at  $300^\circ\text{C}$  in an  $\text{Ar}+\text{NH}_3$  atmosphere gave a mixed-valence vanadium oxide,  $(\text{NH}_4)_x\text{V}_3\text{O}_7$  ( $x \approx 0.6$ ), isostructural with  $\text{Cs}_{0.37}\text{V}_3\text{O}_7$ . The crystal structure of  $(\text{NH}_4)_x\text{V}_3\text{O}_7$  was refined by the Rietveld method (hexagonal,  $P6_3/m$ ,  $a = 9.8436(6)$ ,  $c = 3.6165(1)$  Å,  $V = 303.47(3)$  Å<sup>3</sup>,  $Z = 2$ ).  $(\text{NH}_4)_x\text{V}_3\text{O}_7$  comprises edge- and corner-sharing  $\text{V}^{\text{IV/V}}\text{O}_5$  square-pyramids with an approximate ratio of  $\text{V}^{\text{IV}} : \text{V}^{\text{V}} \approx 0.49 : 0.51$ , to form a columnar cavity along the  $c$ -axis, in which ammonium N atoms are hydrogen-bonded to apical O atoms of the  $\text{V}^{\text{IV/V}}\text{O}_5$  square-pyramids. A reflux of the  $(\text{NH}_4)_x\text{V}_3\text{O}_7$  powder in a 0.6 M LiOH/2-methoxyethanol solution brought about Li-insertion into the columnar cavity without any structural change in the  $\{\text{V}_3\text{O}_7\}$  framework.

Mixed-valence vanadium oxides and vanadium bronzes, which consist of corner- and edge-sharing  $\text{V}^{\text{IV/V}}\text{O}_5$  square-pyramids and/or distorted  $\text{V}^{\text{IV/V}}\text{O}_6$  octahedra, have been investigated concerning their structures<sup>1–4</sup> as well as electronic and magnetic properties.<sup>5–7</sup> Especially, the electrochemical  $\text{Li}^+$ -intercalation/deintercalation properties on vanadium oxides with layered or tunnel-type structures have been studied, because they are candidates as cathode materials for rechargeable lithium batteries.<sup>8–16</sup> Many of these compounds have been prepared by solid state reactions,<sup>4,7</sup> pyrolyses,<sup>2,9,17</sup> hydrothermal reactions,<sup>3,16</sup> and sol-gel techniques,<sup>5,6,8,12,14</sup> using simple vanadium oxides such as  $\text{V}_2\text{O}_5$ ,  $\text{VO}_2$ ,  $\text{V}_2\text{O}_3$ , and  $(\text{NH}_4)\text{VO}_3$  as starting materials. In the present study, a polyoxovanadate,  $[\text{V}_{18}^{\text{IV}}\text{O}_{42}(\text{H}_2\text{O})]^{12-}$ , was used as a precursor of mixed-valence vanadium oxides. Since polyoxovanadates can be regarded as molecular fragments of vanadium oxides with infinite structures, the condensation of  $\text{V}^{\text{IV}}$ -containing polyoxovanadates by pyrolysis at low temperatures may be expected to form novel mixed-valence vanadium oxides. Figure 1 shows the structure of  $[\text{V}_{18}^{\text{IV}}\text{O}_{42}(\text{H}_2\text{O})]^{12-}$  used in this study, where eighteen  $\text{V}^{\text{IV}}\text{O}_5$  square-pyramids are condensed with edge- and corner-sharing into a spherical  $\{\text{V}_{18}\text{O}_{42}\}$  cluster encapsulating a water molecule at the center. This paper describes that the pyrolysis of the ammonium salt of  $[\text{V}_{18}^{\text{IV}}\text{O}_{42}(\text{H}_2\text{O})]^{12-}$  at  $300^\circ\text{C}$  in a  $\text{Ar}+\text{NH}_3$  flow leads to the formation of ammonium trivanadate,  $(\text{NH}_4)_x\text{V}_3\text{O}_7$  ( $x \approx 0.6$ ) possessing a tunnel-type cavity, to allow a  $\text{Li}^+$ -insertion reaction without any change in the framework structure.

## Experimental

$(\text{NH}_4)_{12}[\text{V}_{18}^{\text{IV}}\text{O}_{42}(\text{H}_2\text{O})] \cdot n\text{H}_2\text{O}$  ( $n \approx 11$ ) (**1**) was prepared photochemically by a modification of the procedure for the potassium salt,  $\text{K}_{10}[\text{H}_2\text{V}_{18}^{\text{IV}}\text{O}_{42}(\text{H}_2\text{O})] \cdot 16\text{H}_2\text{O}$ .<sup>18</sup> The pH level of an aqueous solution (20 ml) of  $[\text{NH}_3^+\text{Bu}][\text{V}_4\text{O}_{12}]$  (0.5 g)<sup>19</sup> was adjusted to about

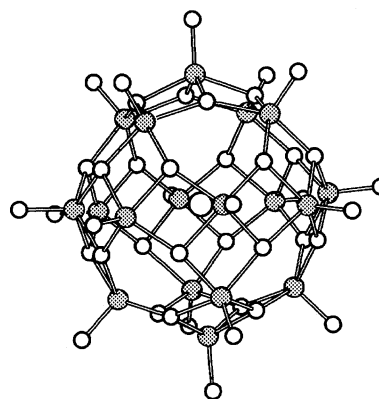


Fig. 1. Structure of  $[\text{V}_{18}^{\text{IV}}\text{O}_{42}(\text{H}_2\text{O})]^{12-}$ .<sup>18</sup> V and O atoms are denoted by shaded and open circles, respectively. The central large open circle represents the water O atom encapsulated by the  $\{\text{V}_{18}\text{O}_{42}\}$  cage.

11 with aqueous ammonia. The resultant solution was mixed with methanol (2 ml), sealed in a Pyrex tube, and then exposed to light from a 500-W super-high-pressure mercury lamp without filtering for about 24 h. After exposure, the tube was kept to cool at room temperature. Dark-brown crystallines of **1** were formed within several days. The vanadium content of **1** was determined thermogravimetrically by conversion to  $\text{V}_2\text{O}_5$  at  $600^\circ\text{C}$  in air. Found: H, 3.61; N, 8.38; V, 44.4%. Calcd for  $(\text{NH}_4)_{12}[\text{V}_{18}\text{O}_{42}(\text{H}_2\text{O})] \cdot 11\text{H}_2\text{O}$ : H, 3.59; N, 8.31; V, 45.36%. The  $\text{V}^{\text{IV}} : \text{V}^{\text{V}}$  ratio in **1** was estimated potentiometrically by direct and back titrations under a  $\text{N}_2$  atmosphere with ammonium iron(II) sulfate and ammonium cerium(IV) sulfate solutions.<sup>18</sup> As a result, **1** consists of only  $\text{V}^{\text{IV}}$ . Since **1** is very air-sensitive to be oxidized, the crystalline solids should be kept in the reaction tube until the following pyrolysis.

A freshly prepared and powdered sample of **1** (0.05 g) was placed on an alumina boat in a quartz tube (diameter: 40 mm) of an electric furnace, and exposed to an  $\text{Ar}+\text{NH}_3$  stream with a flow rate of ca.  $20 \text{ ml min}^{-1}$ . The sample was heated at 200, 250, 300, 350, and

400 °C for 2 h, and cooled to room temperature in the Ar+NH<sub>3</sub> flow. Powder X-ray diffraction (XRD) patterns were measured on a Rigaku RAD-1VB system. The powder pattern for Rietveld refinement<sup>20</sup> was collected on a Rigaku RINT-2000 diffractometer using a step scanning mode with a step width of 0.02° and a counting time of 2 s step<sup>-1</sup>.

## Results and Discussion

**Pyrolysis Products.** XRD patterns of the pyrolysis products are shown in Fig. 2(a)–(e). The pyrolysis of **1** at 200 and 250 °C yielded almost amorphous phases with weak unidentified peaks at  $2\theta = 9$  and  $28^\circ$  (Fig. 2(a) and (b)). At 350 and 400 °C, **1** lost all NH<sub>4</sub><sup>+</sup> cations, to be converted into two VO<sub>2</sub> phases (Fig. 2(d) and (e)). The pyrolysis of **1** at 300 °C resulted in the formation of a new compound (**2**) (Fig. 2(c)).

**Characterization of 2.** The X-ray diffraction angles (Fig. 2(c)) of **2** are in accord with those (Fig. 2(f)) of Cs<sub>0.37</sub>V<sub>3</sub>O<sub>7</sub>,<sup>21</sup> suggesting that **2** is isomorphous with Cs<sub>0.37</sub>V<sub>3</sub>O<sub>7</sub>, to be formulated as (NH<sub>4</sub>)<sub>x</sub>V<sub>3</sub>O<sub>7</sub>. The V<sup>IV</sup>:V<sup>V</sup> ratio and the total V (= V<sup>IV</sup> + V<sup>V</sup>) were determined by the potentiometric titrations with iron(II) and cerium(IV) solutions. The ammonium content (*x*) was estimated to be ca. 0.6 by elemental analysis. Found: H, 0.85; N, 3.13; V, 55.2%. Calcd for (NH<sub>4</sub>)<sub>0.6</sub>V<sub>3</sub>O<sub>7</sub>: H, 0.88; N, 3.05; V, 55.44%. To maintain electrical neutrality, the V<sup>IV</sup>:V<sup>V</sup> ratio should be 0.53:0.47, which is close to 0.49:0.51 obtained by redox titration. Since all vanadium of the starting material (**1**) is V<sup>IV</sup>, the pyrolysis of **1** accompanies the oxidation of V<sup>IV</sup> to V<sup>V</sup>, which was not investigated any further.

The Crystal structure of **2** was refined by the Rietveld method<sup>20</sup> based on the crystallographic parameters of Cs<sub>0.37</sub>V<sub>3</sub>O<sub>7</sub><sup>21</sup> by two different ways. In the first refinement Cs was replaced by ammonium N with the fixed site occupancy of 0.6. This refinement resulted in high convergence factors ( $R_{wp} = 13.85$ ,  $R_p = 10.96$ ,  $S = 3.27$ ,  $R_1 = 9.55$ , and  $R_F = 3.80$ ) with an abnormally long V1–O2 distance (1.743(9) Å) of the V=O<sub>terminal</sub> bonds. On the other hand, in the second refinement, where a part of the V1 atom was disordered as V2 and V3 on the positions of N1 and N2, respectively, low convergence factors ( $R_{wp} = 11.58$ ,  $R_p = 9.14$ ,  $S = 2.74$ ,  $R_1 = 6.21$ ,

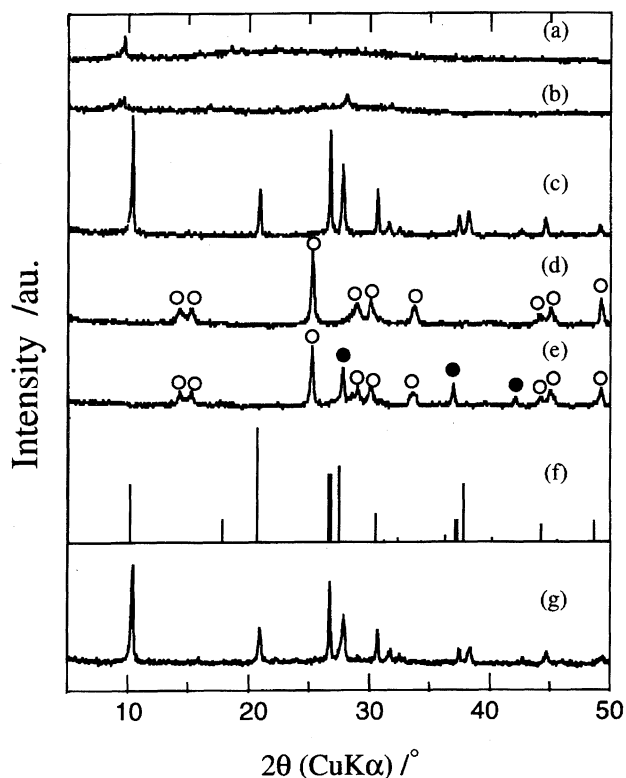


Fig. 2. The XRD patterns of the pyrolysis products of **1** treated at 200 °C (a), 250 °C (b), 300 °C (**2**) (c), 350 °C (d), and 400 °C (e). The patterns of Cs<sub>0.37</sub>V<sub>3</sub>O<sub>7</sub><sup>21</sup> and **2** refluxed in LiOH/2-methoxyethanol solution are shown in (f) and (g), respectively. The open (O) and filled (●) circles in (d) and (e) denote diffraction peaks of two different VO<sub>2</sub> phases.<sup>25,26</sup>

and  $R_F = 2.73$ ) and a reasonable V1–O2 length (1.547(8) Å) were obtained, as shown in Tables 1 and 2. Since the numbers of equivalent positions for V1, V2, and V3 sites in a unit cell are 6, 2, and 2, respectively (Table 1), the site occupancies (Occ's) of the V1–3 atoms were refined under a constraint condition of  $\text{Occ}(\text{V1}) = 1 - \{\text{Occ}(\text{V2}) + \text{Occ}(\text{V3})\}/3$  in order to maintain the V : O = 3 : 7 ratio. Figure 3 shows the observed XRD patterns of **2** and the patterns

Table 1. Structural Parameters of **2** Obtained by Rietveld Refinement

Lattice type, space group: hexagonal,  $P6_3/m$ . Unit cell parameters:  $a = 9.8436(6)$ ,  $c = 3.6165(1)$  Å,  $V = 303.47(3)$  Å<sup>3</sup>.  $R$  factors:  $R_{wp} = 11.58$ ,  $R_p = 9.14$ ,  $R_e = 4.23$ ,  $R_F = 2.73$ .

| Atom | <i>x</i>  | <i>y</i>  | <i>z</i> | Site <sup>a)</sup> | Occ <sup>b)</sup>     | <i>B</i> /Å <sup>2</sup> |
|------|-----------|-----------|----------|--------------------|-----------------------|--------------------------|
| V1   | 0.1218(3) | 0.6227(3) | 1/4      | 6 <i>h</i>         | 0.917 <sup>c)</sup>   | 0.33(8) <sup>d)</sup>    |
| V2   | 0         | 0         | 1/4      | 2 <i>a</i>         | 0.10(1) <sup>c)</sup> | 0.33(8) <sup>d)</sup>    |
| V3   | 0         | 0         | 0        | 2 <i>b</i>         | 0.15(1) <sup>c)</sup> | 0.33(8) <sup>d)</sup>    |
| N1   | 0         | 0         | 1/4      | 2 <i>a</i>         | 0.3                   | 49(16) <sup>e)</sup>     |
| N2   | 0         | 0         | 0        | 2 <i>b</i>         | 0.3                   | 49(16) <sup>e)</sup>     |
| O1   | 0.0951(8) | 0.5537(7) | 3/4      | 6 <i>h</i>         | 1.0                   | 2.6(2) <sup>f)</sup>     |
| O2   | 0.216(1)  | 0.345(1)  | 1/4      | 6 <i>h</i>         | 1.0                   | 2.6(2) <sup>f)</sup>     |
| O3   | 1/3       | 2/3       | 1/4      | 2 <i>c</i>         | 1.0                   | 2.6(2) <sup>f)</sup>     |

a) Wyckoff's notation. b) Site occupancy. c) Refined under a constraint condition of  $\text{Occ}(\text{V1}) = 1 - \{\text{Occ}(\text{V2}) + \text{Occ}(\text{V3})\}/3$  (see text). d) e), f) Refined as common parameters.

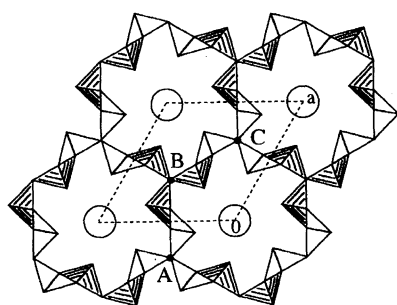
Table 2. V–O Bond Distances (Å) and O–V–O Bond Angles (°) in the VO<sub>5</sub> Square Pyramid<sup>a)</sup>

|                                      |          |                        |          |
|--------------------------------------|----------|------------------------|----------|
| V1–O2 <sup>i</sup>                   | 1.547(8) | V1–O3                  | 1.905(1) |
| V1–O1                                | 1.905(2) | V1–O1 <sup>ii</sup>    | 1.968(6) |
| O2 <sup>i</sup> –V1–O1               | 107.3(2) | O2 <sup>i</sup> –V1–O3 | 106.0(5) |
| O2 <sup>i</sup> –V1–O1 <sup>ii</sup> | 112.5(5) | O1–V1–O1 <sup>ii</sup> | 143.4(4) |
| O1–V1–O1 <sup>ii</sup>               | 78.0(2)  | O3–V1–O1 <sup>ii</sup> | 141.5(3) |
| O1–V1–O3                             | 91.0(2)  |                        |          |

a) Symmetry codes: (i)  $-x+y, 1-x, z$ ; (ii)  $-x, 1-y, -1/2+z$ .

fitted based on the result of a second refinement, indicating that both of the patterns are quite similar. The refined Occ's of V1, V2, and V3 are 0.917, 0.10(1), and 0.15(1), respectively (Table 1), to be formulated as (NH<sub>4</sub>)<sub>0.6</sub>(V<sub>12.75</sub>)(V<sub>20.10</sub>)(V<sub>30.15</sub>)O<sub>7</sub>. However, no further information on the distributions and valence states of V2 and V3 has been obtained. Such a disordering of metal cations in columnar cavities or between host layers has been found in several ternary metal oxides. For example, a columnar cavity in a modified hollandite-type A<sub>2-*x*</sub>V<sub>8+2*x*</sub>O<sub>16+*x*</sub> (A = K, Rb) accommodates not only A cations, but also V cations.<sup>22</sup> In the case of LiFeO<sub>2</sub>, as another example, Fe<sup>3+</sup> in {FeO<sub>2</sub>} layers and Li<sup>+</sup> between {FeO<sub>2</sub>} layers are partially exchanged with a disorder, to be formulated as Li<sub>0.907</sub>(Li<sub>0.093</sub>)FeFe<sub>0.907</sub>(Fe<sub>0.093</sub>)LiO<sub>2</sub>.<sup>23</sup> Similarly, in a non-stoichiometric LiNb<sub>1+*x*</sub>O<sub>3</sub> (*x* = 0.008–0.128), a part of the Li<sup>+</sup> cations is replaced by Nb<sup>5+</sup> cations to form Li<sup>+</sup> vacancies as the result of charge compensation.<sup>24</sup>

Figure 4(a) shows the structure of **2** viewed from the *c*-axis. The {V<sub>3</sub>O<sub>7</sub>} framework in the hexagonal lattice comprises edge- and corner-shared VO<sub>5</sub> square-pyramids, and



(a)

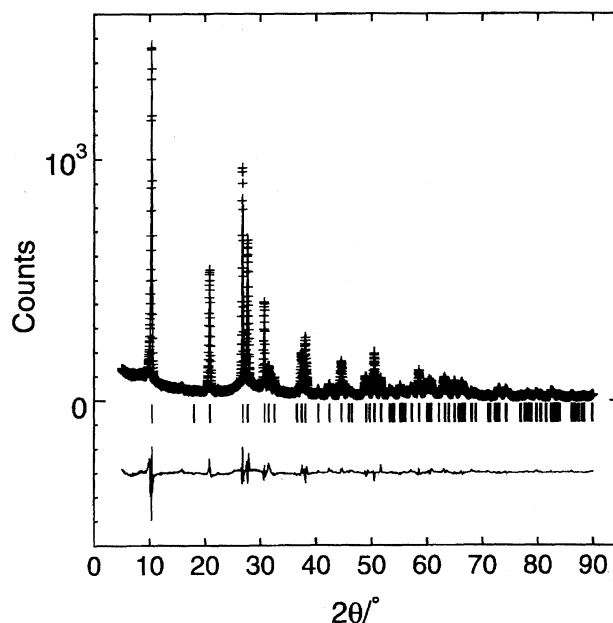
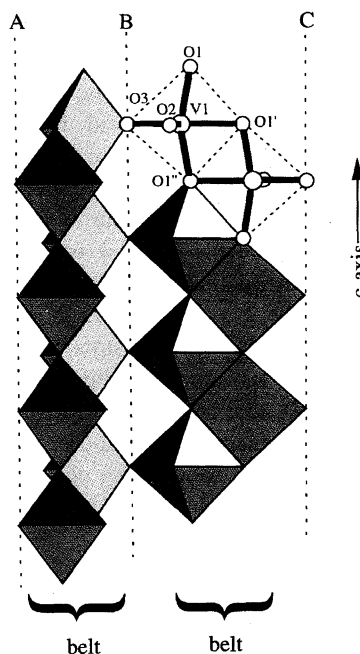


Fig. 3. Observed (+) and fitted (—) XRD patterns of **2** refined by Rietveld method.<sup>20</sup> The vertical bars denote calculated diffraction angles. The pattern at bottom denotes differences between observed and calculated intensities.

possesses a columnar cavity along the *c*-direction. Figure 4(b) shows a side view (perpendicular to the *c*-direction) of the {V<sub>3</sub>O<sub>7</sub>} lattice, where the broken lines A, B, and C correspond to points A, B, and C in Fig. 4(a). As shown in Fig. 4(b), the O2 atom and [O1, O1', O1'', O3] square form an apex and a basal plane of the VO<sub>5</sub> square-pyramid, respec-



(b)

Fig. 4. Polyhedral representation of the crystal structure of **2** viewed parallel (a) and perpendicular (b) to the *c*-axis. Two of the VO<sub>5</sub> square-pyramids in (b) are drawn by ball and stick model. The points A, B, and C in (a) correspond to the dashed lines A, B, and C in (b), respectively.

tively. The VO<sub>5</sub> polyhedra are connected by edge-sharing along the *c*-direction to form a belt structure (Fig. 4(b)). One columnar cavity is made up of six belts by corner-sharing through O3 atoms with a hexagonal configuration (Fig. 4(a)). It is noteworthy that the same belt structure can be found in layer-structural V<sub>2</sub>O<sub>5</sub> and M<sub>x</sub>V<sub>2</sub>O<sub>5</sub> (M = alkaline or alkaline earth metals) bonzes.<sup>1</sup> Table 2 summarizes the bond distances and angles for the VO<sub>5</sub> square-pyramid, which are similar to those for isostructural Cs<sub>0.37</sub>V<sub>3</sub>O<sub>7</sub>.<sup>21</sup> The ammonium N atoms in the columnar cavities are hydrogen-bonded to the terminal O2 atoms at N...O distances of 2.980(9)—3.114(8) Å.

There have been several methods for the preparation of vanadium oxides and vanadium bronzes by pyrolysis of NH<sub>4</sub>VO<sub>3</sub> in a reducing or inert gas atmosphere. For example, the decomposition of NH<sub>4</sub>VO<sub>3</sub> solids in H<sub>2</sub> flow at 230 °C yields β-(NH<sub>4</sub>)<sub>x</sub>V<sub>2</sub>O<sub>5</sub> (*x* ≈ 0.38) consisting of host {V<sub>2</sub><sup>IV/V</sup>O<sub>5</sub>} layers and NH<sub>4</sub><sup>+</sup> cations.<sup>17</sup> VO<sub>2</sub> with a tunnel-structure has been prepared by the pyrolysis of NH<sub>4</sub>VO<sub>3</sub> at 330 °C in NH<sub>3</sub> stream.<sup>9</sup> Also, NH<sub>4</sub>VO<sub>3</sub> was converted to layer-structural V<sub>6</sub>O<sub>13-y</sub> by decomposition at 500—550 °C in an Ar stream.<sup>15</sup> The pyrolyses of NH<sub>4</sub>V<sup>VO</sup>O<sub>3</sub> or V<sup>IV</sup>OSO<sub>4</sub> at 200—400 °C under Ar+NH<sub>3</sub> atmosphere exhibited no formation of **2**, suggesting that the formation of **2** is characteristic of the pyrolysis of **1**. This renders the fact that both the VO<sub>5</sub> square-pyramids and the ratio of V : O = 3 : 7 are common to the anion frameworks of {V<sub>18</sub>O<sub>42</sub>} in **1** and {V<sub>3</sub>O<sub>7</sub>} in **2**. We are actively pursuing the pyrolysis of the polyoxovanadates with other structures and compositions to address a preparative novel vanadium oxides.

**Li Insertion into 2.** The insertion of Li<sup>+</sup> into a columnar cavity occurred by the reflux of **1** (0.15 g) in 0.6 M LiOH/2-methoxyethanol (1 M = 1 mol dm<sup>-3</sup>) solutions (20 ml) for 2 h. The product was collected by filtration, washed with 2-methoxyethanol, and dried in air. An elemental analysis showed the V/Li ratio to be ca. 2.9 (observed; H, 1.40; Li, 2.30; N, 1.91; V, 48.1%). The V<sup>IV</sup> : V<sup>V</sup> ratio (ca. 0.45 : 0.55) was nearly the same as that (0.49 : 0.51) for **2**. The XRD pattern is shown in Fig. 2(g), which is similar to the pattern of **2** (Fig. 1(c)), indicating that the {V<sub>3</sub>O<sub>7</sub>} framework is retained through the Li-insertion reaction. The *a* (= *b*) axis was ca. 0.05 Å less than for **2**, probably due to the small size of Li<sup>+</sup> compared to NH<sub>4</sub><sup>+</sup>. These results suggest the approximate formula of the Li-insertion product to be Li-(OH)(H<sub>2</sub>O)(NH<sub>4</sub>)<sub>0.4</sub>V<sub>3</sub>O<sub>7</sub> (Calcd for: H, 1.48; Li, 2.21; N, 1.78; V, 48.67%). The existence of OH<sup>-</sup> and/or H<sub>2</sub>O was also suggested by IR absorption bands (data not shown) at ca. 1600 and ca. 3400 cm<sup>-1</sup>, which are assigned to ν(OH) and δ(HOH) vibrations, respectively.<sup>27</sup>

This work was supported in part by a Grant-in-Aid for Scientific Research on Priority Areas (No. 260) from the Ministry of Education, Science, Sport and Culture. The authors express their thanks to Professor M. Wakihara and Dr.

H. Ikuta for providing facilities for X-ray powder diffraction measurement.

## References

- 1 J. Galy, *J. Solid State Chem.*, **100**, 229 (1992).
- 2 J. M. Savariault and J. Galy, *J. Solid State Chem.*, **101**, 119 (1992).
- 3 Y. Zhang, R. C. Haushalter, and A. Clearfield, *J. Chem. Soc., Chem. Commun.*, **1996**, 1055.
- 4 A. Hardy, J. Galy, A. Casalot, and M. Pouchard, *Bull. Soc. Chim. Fr.*, **4**, 1056 (1965).
- 5 J. C. Badot, D. Gourier, F. Bourdeau, N. Baffier, and A. Tabuteau, *J. Solid State Chem.*, **92**, 8 (1991).
- 6 J. C. Badot and N. Baffier, *J. Solid State Chem.*, **93**, 53 (1991).
- 7 M. Isobe and Y. Ueda, *J. Alloys Comp.*, **262-263**, 180 (1997).
- 8 K. West, B. Zachau-Christiansen, S. Skaarup, Y. Saidi, J. Barker, I. I. Olisen, R. Pynenburg, and R. Koksang, *J. Electrochem. Soc.*, **143**, 820 (1996).
- 9 M. Zhang and J. R. Dohn, *J. Electrochem. Soc.*, **143**, 2730 (1996).
- 10 H. Groult, D. Devilliers, N. Kumagai, J. Nakajima, and M. Matsuo, *J. Electrochem. Soc.*, **143**, 2093 (1996).
- 11 B. Pecquenard, D. Gourier, and N. Baffier, *Solid State Ionics*, **78**, 287 (1995).
- 12 K. Salloux, F. Chaput, H. P. Wong, B. Dunn, and M. W. Breiter, *J. Electrochem. Soc.*, **142**, L191 (1995).
- 13 M. Ugaji, M. Hibino, and T. Kudo, *J. Electrochem. Soc.*, **142**, 3664 (1995).
- 14 G. Pistoia, M. Pasquali, G. Wang, and L. Li, *J. Electrochem. Soc.*, **137**, 2365 (1990).
- 15 D. W. Murphy, P. A. Christian, F. J. Disalvo, J. N. Carides, and J. V. Waszczak, *J. Electrochem. Soc.*, **128**, 2053 (1981).
- 16 T. A. Chirayil, P. Y. Zavalij, and M. S. Whittingham, *J. Electrochem. Soc.*, **143**, L193 (1996).
- 17 T. Palanisamy, J. Gopalakrishnan, and M. V. C. Sastri, *J. Solid State Chem.*, **9**, 273 (1974).
- 18 T. Yamase, K. Ohtaka, and M. Suzuki, *J. Chem. Soc., Dalton Trans.*, **1996**, 283.
- 19 P. Róman, A. San José, A. Luque, and J. M. Gutiérrez-Zorrilla, *Inorg. Chem.*, **32**, 775 (1993).
- 20 F. Izumi, "The Rietveld Method," ed by R. A. Young, Oxford Press, Oxford (1993), Chap. 13.
- 21 K. Waltersson and B. Forslund, *Acta Crystallogr., Sect. B*, **B33**, 775 (1977).
- 22 W. Abriel, C. Garbe, F. Rau, and K. -J. Range, *Z. Kristallogr.*, **176**, 113 (1986).
- 23 R. Kanno, T. Shirane, Y. Kawamoto, Y. Takeda, M. Takano, M. Ohashi, and Y. Yamaguchi, *J. Electrochem. Soc.*, **143**, 2435 (1996).
- 24 N. Iyi, K. Kitamura, F. Izumi, J. K. Yamamoto, T. Hayashi, H. Asano, and S. Kimura, *J. Solid State Chem.*, **101**, 340 (1992).
- 25 JCPDS, *X-Ray Powder Data File*, card 31-1438.
- 26 JCPDS, *X-Ray Powder Data File*, card 9-0142.
- 27 A. Müller, J. Döring, M. I. Khan, and V. Wittneben, *Angew. Chem., Int. Ed. Engl.*, **30**, 210 (1991).